

# Enhanced Photocurrent Generation in Self-Assembled Monolayers Formed at Plasmonic Gold Nanostructures

Tsuyoshi Akiyama,<sup>\*1,2</sup> Masato Nakada,<sup>2</sup> Kosuke Sugawa,<sup>2</sup> Sunao Yamada<sup>1,2,3</sup>

**Summary:** The effect of localized surface plasmon resonance (SPR) appearing at the surfaces of gold nanoparticles (AuPs) was successfully applied for the enhancement of photocurrents from porphyrin (**Po**) immobilized on AuPs. The electrode consisting of AuPs with different sizes ( $\sim 15$  or  $\sim 35$  nm) was prepared using the AuP film formed at the liquid/liquid interface, and then **Po** was self-assembled on the gold surface. The SPR effect for the AuP film was verified from the attenuated total reflection SPR and absorption measurements. Photocurrents from the modified electrodes were compared with the corresponding planar electrode. Appreciable enhancement of photocurrents was observed.

**Keywords:** bottom-up nanofabrication; nanoparticles; photocurrent; plasmon; surfaces

## Introduction

Surface plasmon resonance (SPR) appearing at the surface of noble-metal (especially gold and silver) will open-up unique applications of light at nano-scales, because the group velocity of light will be lowered and the strong electric field resulting from the incidence of light will be produced at specified local regions of the metal surface. As typical examples, electronic excitation of surface-anchored molecules has been enhanced, as has been verified from the enhancements of fluorescence [1–8] and photocurrent [9–12] signals. Thus, SPR can offer tremendous advantages in the spectroscopic sensitivity. However, as to the SPR method reported so far, optical excitation of surface plasmon waves, relevant to the excitation of surface-anchored molecules, has been carried out under the attenuated total reflection geometry using a planar surface.

Surface plasmon on the surfaces of gold (or silver) nanoparticles has made it possible to extremely enhance the sensitivity in the Raman scattering spectroscopy as a surface-enhanced Raman scattering (SERS).<sup>[13]</sup> Such an enhancement in optical events must extend the applications of surface plasmon in various spectroscopies. The primary importance for these applications is skillful design and tailor-made fabrication of gold (or silver) metal nanostructures. We preliminarily reported the photocurrent enhancement in organic dyes that were immobilized on the surface of gold nanoparticles (AuPs).<sup>[14–16]</sup> In this paper, we will describe the effects of the size of gold nanoparticle on the photocurrent enhancement from the self-assembled monolayer (SAM) of porphyrin (**Po**) formed at the surfaces of AuP films prepared at the liquid/liquid interface.

## Experimental Part

The gold nanoparticles with  $\sim 15$ - and  $\sim 35$ -nm mean diameters, denoted as AuP(15) and AuP(35), were prepared according to the previous method.<sup>[13]</sup> The preparation of AuP films at the liquid/liquid interface is shown in Figure 1.<sup>[17]</sup> Namely, the liquid/liquid interface of the aqueous colloidal

<sup>1</sup> Department of Materials Physics and Chemistry, Graduate School of Engineering, Kyushu University, Moto-oka 744, Nishi-ku, Fukuoka 819-0395, Japan  
E-mail: t-akitem@mbox.nc.kyushu-u.ac.jp

<sup>2</sup> Department of Applied Chemistry, Graduate School of Engineering, Kyushu University, Moto-oka 744, Nishi-ku, Fukuoka 819-0395, Japan

<sup>3</sup> Center for Future Chemistry, Kyushu University, Moto-oka 744, Nishi-ku, Fukuoka 819-0395, Japan

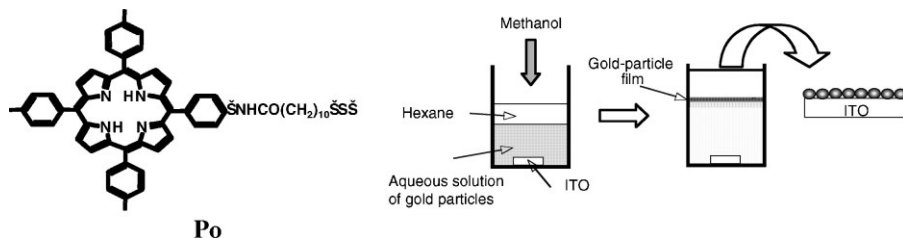


**Figure 1.**

Schematic illustration for the preparation of gold-nanoparticle film at the liquid-liquid interface.

solution of AuPs (20 ml) and hexane (10 ml) was formed in a vial, and an indium-tin-oxide (ITO) electrode was placed at its bottom. Next, methanol (10 ml) was poured into the solution at once, resulting the generation of liquid-like film of AuPs at the liquid/liquid interface. Then, this liquid-like film was carefully transferred onto the surface of the ITO electrode. Accordingly, we have obtained the multistructured electrode with the gold nanoparticles, denoted as ITO/AuP. Meanwhile, a planar gold electrode was prepared by vacuum deposition of gold onto the ITO electrode, denoted as ITO/Au.

A disulfide derivative of porphyrin ( $[\text{Po}]_2$ ) was synthesized in our laboratory.<sup>[13]</sup> Self-assembled monolayers of **Po** (as monomer unit) on the ITO/AuP and ITO/Au were prepared by immersing the electrodes into a  $\text{CH}_2\text{Cl}_2$  solution of **Po** ( $1 \times 10^{-3}$  M) for five days, to obtain **Po**-modified electrodes as: ITO/AuP/**Po** and ITO/Au/**Po**, respectively.

Scanning electron micrograph (SEM) measurement was carried out by Hitachi S-5000. Absorption spectra were recorded on a JASCO V-570 spectrophotometer and SHIMADZU UV-2500PC.

Photocurrents from ITO/AuP/**Po** and ITO/Au/**Po** were measured in an aqueous 0.1 M  $\text{NaClO}_4$  solution under aerobic condition at room temperature, using a three-electrode photoelectrochemical cell (modified electrode as working, Ag/AgCl electrode as reference and platinum electrode as counter). The monochromated light from a Xe lamp irradiated the modified electrode. Stable and static photocurrents

were generated in all cases. Photocurrents were detected by a potentiostat. All measurements were carried out at room temperature.

SPR measurements were carried out by standard attenuated total reflection (ATR) geometry using a home-made system; detailed experimental set-up will appear elsewhere.<sup>[18]</sup>

## Results and Discussion

Highly-sensitive detection of photocurrents at the modified electrodes is essentially important for a variety of photochemical, photophysical, and photobiological studies. Thus the construction of multistructures of AuPs at the planar electrodes is very useful for increasing the active surface area of the electrodes. Figure 2 shows the scanning electron micrograph (SEM) images of the ITO/AuP(15)/**Po** and ITO/AuP(35)/**Po**, respectively. In both cases the AuPs are snugly gathered in macroscopic point of view. Although some of nonspherical particles are seen in the case of AuP(35), their contents are substantially low and thus we did not take into consideration of the effects of those nonspherical particles. Slight fusion of particles is observed, though the reason is not apparent at this stage.

In order to verify the occurrence of SPR event in the AuP film, we have preliminarily investigated the SPR experiment for the AuP(15) film. Figure 3 show the experimental geometry and the resultant SPR profile from the film fixed at the surface of titanium-deposited glass substrate (the

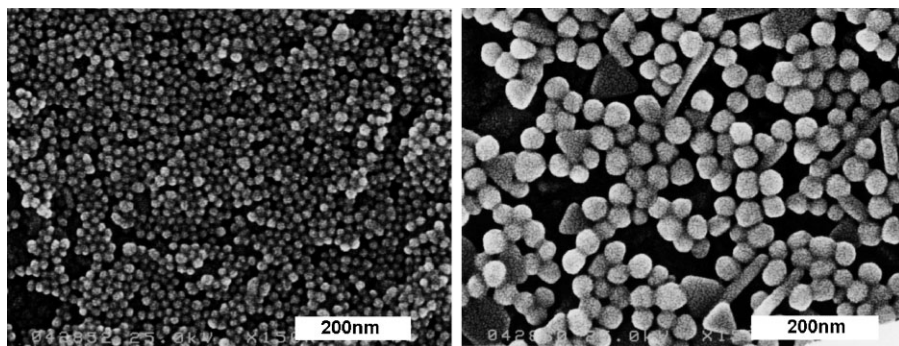


**Figure 2.**

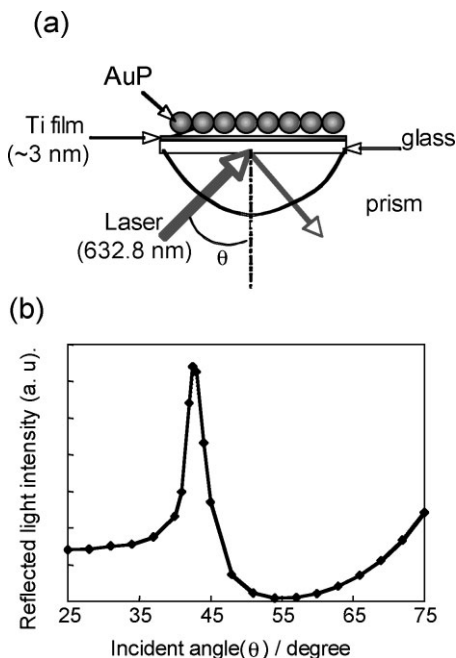
SEM images of ITO/AuP(15) (left) and ITO/AuP(35) (right).

titanium film was necessary to avoid peel-off the AuP film); the reflected light of parallel-polarized He-Ne laser light (632.8 nm) by ATR mode, was measured as a function of the incident angle. It is clear that the reflected light decreased above 45° incident

angle and showed a minimum around 55°. The result indicates that SPR is certainly occurring for the AuP(15) film above 45°.

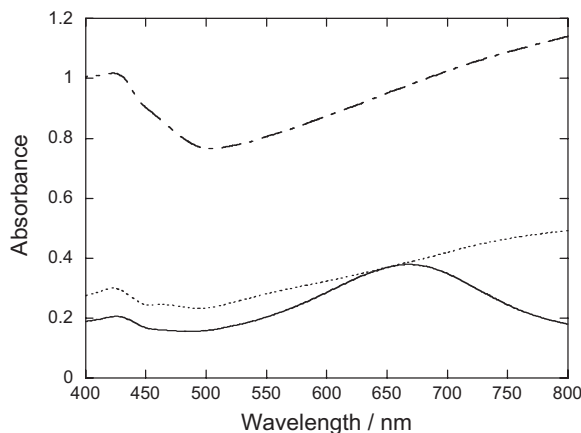
The SPR result is quite consistent with the absorption spectrum as shown in Figure 4, where the broad and red-shifted plasmon band due to the effect of inter-particle plasmon coupling is seen in the 500–800-nm region, as compared with the plasmon band in water (520 nm). ITO/AuP(35)/**Po** also showed a broad plasmon band in the similar wavelength region, whereas the plasmon band of AuP(35) in water was 530 nm. On the other hand, no appreciable bands were seen in ITO/Au/**Po** above 500 nm. These results indicate that the excitation of molecules immobilized on the AuP film by SPR must be possible, as has been suggested previously.<sup>[14,15]</sup> In all modified electrodes, small absorption peaks due to the Soret band of **Po** were also observed, though they were too weak to evaluate the surface coverages of **Po**.

Figure 5 shows photocurrent action spectra of ITO/AuP(15)/**Po**, ITO/Au(35)/**Po**, and ITO/Au/**Po**, respectively. It is clear that the use of AuPs resulted in the increase of photocurrent as compared with the planar electrode: ITO/Au/**Po**. In addition, ITO/AuP(15)/**Po** gave more than one order of magnitude larger photocurrents than ITO/AuP(35)/**Po** and ITO/Au/**Po**. Unfortunately, it was difficult to quantitatively compare the intensities of photocurrents among the three electrodes, because the



**Figure 3.**

Schematic illustration for the measurement of SPR on gold nanoparticle film (a) and a typical SPR profile for AuP(15) as the function of incident angle of laser light (b).



**Figure 4.**

Absorption spectra of ITO/AuP(15)/Po (—), ITO/AuP(35)/Po (-----), and ITO/Au/Po (---).

absorption intensities of **Po** were very small. Thus, we have compared the wavelength profile of relative photocurrent intensities in Figure 5. It is clear that the photocurrents were certainly relatively higher than the planar electrode in the longer wavelength region of  $> \sim 500$  nm where the plasmon bands of AuP films appeared.

In order to verify these tendencies, we have obtained the ratios of photocurrents from the AuP-modified electrodes to the planar electrode as a function of wavelength, as shown in Figure 6. If the photocurrent intensity is only affected by the surface coverage of **Po**, the ratio of photocurrent must reflect the ratio of

surface coverage, and should be independent of wavelength. However, the photocurrent ratio was dependent on the wavelength, and tended to be correlated with the plasmon bands of AuPs. These results strongly indicate the enhancement of photocurrents is caused by using the AuPs because the lowering of group velocity of light as well as enhancement of local electric field are superior to the planar gold surface. In addition, the degree of photocurrent enhancement is more prominent in AuP(15) film where the plasmon band of the film appears more clearly.

Since the photocurrent at  $E = 0$  V vs. Ag/AgCl were observed in the cathodic

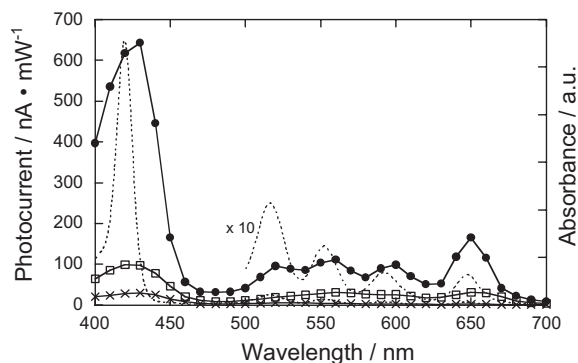


**Figure 5.**

Photocurrent action spectra of ITO/AuP(15)/Po (●), ITO/AuP(35)/Po (□), and ITO/Au/Po (×), and the absorption spectrum of **Po** in dichloromethane (-----).

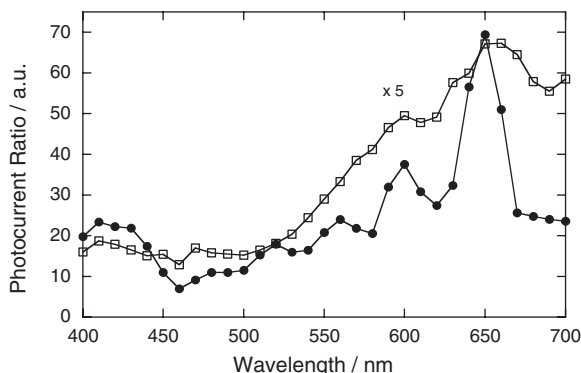


**Figure 6.**

Photocurrent ratios of ITO/AuP(15)/Po versus ITO/Au/Po (●) and of ITO/AuP(35)/Po (□) versus ITO/Au/Po.

direction, the photocurrent generation mechanism is expressed in Figure 7.

First, photoinduced electron-transfer from the photoexcited Po ( $^*\text{Po}$ ) to  $\text{O}_2$  initiates the electron flow. Then, AuPs give the electron to the oxidized Po ( $\text{Po}^+$ ), giving the overall photocurrent flow in the cathodic direction. It is suggested that the concomitant photoexcitation of AuPs induce strong electronic fields around the gaps of AuPs that may additionally contribute to photoexcitation of Po. Accordingly, photocurrents were relatively larger in the wavelength region of SPR in ITO/AuP/Po.

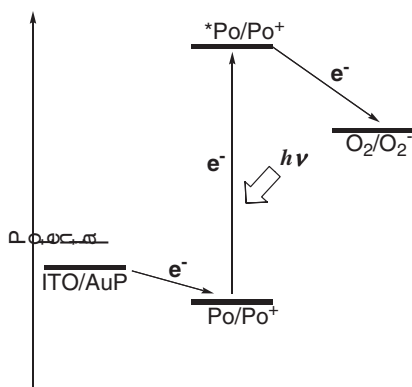


**Figure 7.**

Photocurrent generation mechanism including the path of electron flow. The redox potentials of Po and oxygen are cited from references.

## Conclusion

We have demonstrated that the SPR effect enhanced photocurrent generation from Po immobilized on the surface of AuPs and the degree of enhancement tended to be higher for the AuP film having clear plasmon peak. Such a photocurrent enhancement must be very useful for increasing the sensitivity in photoelectrochemistry.

**Acknowledgements:** The present study was partially supported by a Grant-in-Aid for Scientific Research (No. 19049012) on Priority Area “Strong Photons-Molecules Coupling Fields (470) from the Ministry of Education, Culture, Sports, Science and Technology (MEXT) of the Japan.

- [1] R. E. Benner, R. Dornhaus, R. K. Chang, *Opt. Commun.* **1979**, 30, 145.
- [2] J. W. Attridge, P. B. Daniels, J. K. Deacon, G. A. Robinson, G. P. Davidson, *Biosens. Bioelectron.* **1991**, 6, 201.
- [3] H. Knobloch, H. Brunner, A. Leitner, F. Aussenegg, W. Knoll, *J. Chem. Phys.* **1993**, 98, 10093.
- [4] S. C. Kitson, W. L. Barnes, J. R. Sambles, N. P. K. Cotter, *J. Mod. Opt.* **1996**, 43, 573.
- [5] H. Kano, S. Kawata, *Opt. Lett.* **1996**, 21, 1848.
- [6] A. Ishida, Y. Sakata, T. Majima, *Chem. Commun.* **1998**, 57.
- [7] A. Ishida, T. Majima, *Analyst*, **2000**, 125, 535.
- [8] T. Liebermann, W. Knoll, *Colloids Surf. A* **2000**, 171, 115.
- [9] A. Ishida, Y. Sakata, T. Majima, *Chem. Lett.* **1998**, 267.
- [10] A. Ishida, T. Majima, *Chem. Phys. Lett.* **2000**, 322, 242.

- [11] N. Fukuda, M. Mitsuishi, A. Aoki, T. Miyashita, *Chem. Lett.* **2001**, 378.
- [12] N. Fukuda, M. Mitsuishi, A. Aoki, T. Miyashita, *J. Phys. Chem. B* **2002**, 106, 7048.
- [13] M. Suzuki, Y. Niidome, Y. Kuwahara, N. Terasaki, K. Inoue, S. Yamada, *J. Phys. Chem. B* **2004**, 108, 11660.
- [14] N. Terasaki, S. Nitahara, T. Akiyama, S. Yamada, *Jpn. J. Appl. Phys.* **2005**, 44, 2795.
- [15] T. Akiyama, M. Nakada, N. Terasaki, S. Yamada, *Chem. Commun.* **2006**, 395.
- [16] N. Terasaki, N. Yamamoto, T. Hiraga, I. Sato, Y. Inoue, S. Yamada, **2006**, 499, 153–156.
- [17] M. Suzuki, Y. Niidome, N. Terasaki, K. Inoue, Y. Kuwahara, S. Yamada, *Jpn. J. Appl. Phys.* **2004**, 43, 554.
- [18] K. Sugawa, T. Akiyama, S. Yamada, to be submitted.